Detection of Schistosoma haematobium using lensless imaging and flow cytometry, a proof of principle study

Agbana, Tope; Nijman, Patrick; Hoeboer, M.D.B.; van Grootheest, D.N.; van Diepen, Angela; van Lieshout, Lisette; Diehl, Jan-Carel; Verhaegen, Michel; Vdovin, Gleb

DOI
10.1117/12.2545220

Publication date
2020

Document Version
Final published version

Published in
Proceedings of SPIE

Citation (APA)
Agbana, T., Nijman, P., Hoeboer, M. D. B., van Grootheest, D. N., van Diepen, A., van Lieshout, L., Diehl, J.-C., Verhaegen, M., & Vdovin, G. (2020). Detection of Schistosoma haematobium using lensless imaging and flow cytometry, a proof of principle study. In G. L. Coté (Ed.), *Proceedings of SPIE: Optical Diagnostics and Sensing XX: Toward Point-of-Care Diagnostics* (Vol. 11247). Article 112470F (Progress in Biomedical Optics and Imaging - Proceedings of SPIE; Vol. 11247). SPIE. https://doi.org/10.1117/12.2545220

Detection of Schistosoma haematobium using lensless imaging and flow cytometry, a proof of principle study

Agbana, Temitope, Nijman, Patrick, Hoeber, Max, van Grootheest, Derk, van Diepen, Angela, et al.

Temitope Agbana, Patrick Nijman, Max Hoeber, Derk van Grootheest, Angela van Diepen, Lisette van Lieshout, Jan-Carel Diehl, Michel Verhaegen, Gleb Vdovine, "Detection of Schistosoma haematobium using lensless imaging and flow cytometry, a proof of principle study," Proc. SPIE 11247, Optical Diagnostics and Sensing XX: Toward Point-of-Care Diagnostics, 112470F (14 February 2020); doi: 10.1117/12.2545220

SPIE.

Event: SPIE BiOS, 2020, San Francisco, California, United States

Detection of Schistosoma haematobium using lensless imaging & flow cytometry, a proof of principle study

Temitope Agbana[a], Patrick Nijman[a], Max Hoeboer[b], Derk van Grootheest[a], Angela van Diepen[c], Lisette van Lieshout[c], Jan-Carel Diehl[b], Michel Verhaegen[a], and Gleb Vdovine[a]

[a]Delft University of Technology, Delft Center for Systems and Controls, Delft, 2628CD,The Netherlands

[b]Delft University of Technology, Sustainable Design Engineering, IDE, Delft, 2628CE,The Netherlands

[c]Leiden University Medical Center, Department of Parasitology, Leiden, 2300RC, The Netherlands

ABSTRACT

We present a simple method for the diagnosis of urinary schistosomiasis using an in-line lensless holographic microscope combined with flow cytometry technique. Using simple image processing algorithms and binary image classifier, our system provides automated detection of *Schistosoma haematobium* eggs in infected urine samples. Registered hologram is reconstructed by applying backpropagation from sensor to sample plane and reconstructed image is automatically analysed for the presence of *S. haematobium* eggs. Designed for use in a resource-poor laboratory setting, our proposed method has been implemented using a Raspberry Pi computer. From pre-clinical test performed with human urine samples spiked with *S. haematobium* eggs (approximately 200 eggs per 12 ml of urine), we achieved a sensitivity and specificity of 50.6% and 98.6% respectively. Our proposed method requires no complex sample preparation methods making the system simple to operate and useable in point-of-care diagnosis of urinary schistosomiasis.This method can be optimized to complement existing diagnostic procedures for the detection of *S. haematobium* eggs and can be deployed to inaccessible remote areas.

Keywords: *Schistosoma haemtobium*, digital holography, flow cytometry, neglected tropical disease

1. INTRODUCTION

Schistosomiasis is a neglected tropical disease that affects over 250 million people worldwide with about 779 million people at risk. It predominantly plagues the population living in deprived areas with poor access to clean water and adequate sanitation.[1–4] About 80% of the yearly infections are among the rural dwellers in tropical Sub-Saharan African countries where access to clinical diagnostic instruments is practically limited. Accurate and reliable diagnosis is not only important for patient treatment but also critical for effective and efficient implementation of control and elimination strategy.[5] *S. haematobium, S.mansoni, and S.japonicum* are three well-known species, in this research work however, we focus on the rapid diagnosis of *S. haematobium* in urine samples. The choice is due to the fact that a urine sample is a more simple material to obtain and process.[3,5] Also, developing an algorithm for the detection of relatively large structures that are typically not present in normal urine is easily achievable. Compared to feaces in which the eggs from the other species can be detected, urine is a more cleaner sample to work with.

Microscopic examination of *S.haematobium* eggs in urine sample using filtration, sedimentation or centrifugation techniques is the traditional method used for the diagnosis of an infected individual. The use of hand-held microscopes and cellphone-based microscopes for the diagnosis of *S. haematobium* and other parasitic diseases in field settings has been widely reported in literature.[5–10] The portability, ease-of-use and relatively low cost make this diagnostic technique attractive for the application in resource poor settings. The performance of

Further author information: (Send correspondence to Temitope E. Agbana.)
Temitope E. Agbana.: E-mail: t.e.agbana@tudelft.nl, Telephone: +31152785305
Jan Carel Diehl: E-mail: J.C.Diehl@tudelft.nl, Telephone: +31152789729

Optical Diagnostics and Sensing XX: Toward Point-of-Care Diagnostics, edited by Gerard L. Coté, Proc. of SPIE Vol. 11247, 112470F · © 2020 SPIE · CCC code: 1605-7422/20/$21 · doi: 10.1117/12.2545220

these lens-based imaging techniques is however limited by two critical factors : (i) robustness of the imaging system, (ii) the required manual demand of sample preparation, analysis and documentation of test results. Possible misalignment of the optics, system complexity and required technical expertise for system repairs and maintenance constitute potential limitations to the robustness of the imaging system. Cost, wide availability of recommended urine filters, power requirement of centrifuge on the field, need for sample staining and delays due to sedimentation are common factors that increase the complexity of conventional sample preparation procedures on the field.

In this work, we propose a simple, robust, easy-to-use and automated image based technique that could potentially address the above limitations using the combination of lens-less imaging and flow cytometry. The proposed method completely alleviates the burden, cost and complexity of the sample preparation methods. Automated detection, classification and counting of eggs has been achieved by use of deep learning classification routines combined with simple image processing methods. Due to the achieved minimal computational complexity the developed AI model runs smoothly on simple, low-cost general computers such as Raspberry Pi. The developed model could enable automated diagnosis which can potentially reduce manual labour. Design considerations and steps for a functional, robust and interactive prototype with mapping potentials for field test is also reported. To the best of our knowledge, no similar diagnostic method for urinary schistosomiasis has been reported in literature. In this paper, we outline the methodology, design and operational principles of our proposed diagnostic system.

2. THEORETICAL DETAILS

This section provides a quick overview of the theoretical principle of Digital inline Holographic Microscopes. Flow cytometery technique is also quickly described to the extent to which it applies to our work.

2.1 Principles of Digital inline Holography Microscopes (DIHM)

Lensless imaging is a good option for the design and development of point-of-care devices for global health application.[11–13] It uses a digital sensor to directly sample the light transmitted through a specimen without the use of any imaging lenses.[14,15] Its relative advantages over conventional lens-based microscopes include a larger field of view (FoV), decoupling of FoV from achievable spatial resolution, increased robustness and cost-effectiveness. Bright-field lens-free microscopes are largely categorized into contact-mode shadow imaging–based microscopes and diffraction-based lens-free microscopes. In the contact-mode shadow imaging-based technique, diffraction is reduced by minimizing the sample to sensor distance (typically less than 1μm). Linder et al[16] applied this on-chip imaging method for the detection of *S. haematobium* eggs by simply placing residue of centrifuged urine directly on CMOS sensors and applying computer vision to detect *S. haematobium* eggs present. The method achieves a spatial resolution that is sufficient for egg detection. However, modifying the hardware and replacing the camera sensor after every measurement increases the cost and technical requirement for maintaining such a system. Also, the need to centrifuge or sediment the urine sample increases the complexity of the sample preparation method on the field.

Our approach is based on diffraction-based lens-free Digital Inline Holography Microscopes (DIHMs). In in-line holography a spherical wave of wavelength λ, emanating from a monochromatic point source illuminates a sample as shown in Fig 1.

As a result of the coherent optical field impinging on the sample plane, the shadows registered by the CCD exhibit interference fringe patterns. The fringe pattern is as a result of the interference between light scattered from an object on the sample and a reference wave that passes undisturbed through a transparent glass slide. The electric field at the plane where the reference and object light waves interact can be described as the sum of the reference wave , E_R, s , and the object wave E_O, s as shown in equation below,

$$Es = E_{R,s} + E_{O,s} = \psi_R + \psi_O(x_s, y_s)e^{i\phi_O(x_s,y_s)}, \tag{1}$$

where ψ_R is the amplitude of the reference wave, $\psi_O(x_s, y_s)$ is the spatially varying amplitude (transmittance) of the object, and $\phi_O(x_s, y_s)$ is the spatially varying phase (optical thickness) of the object. The complex

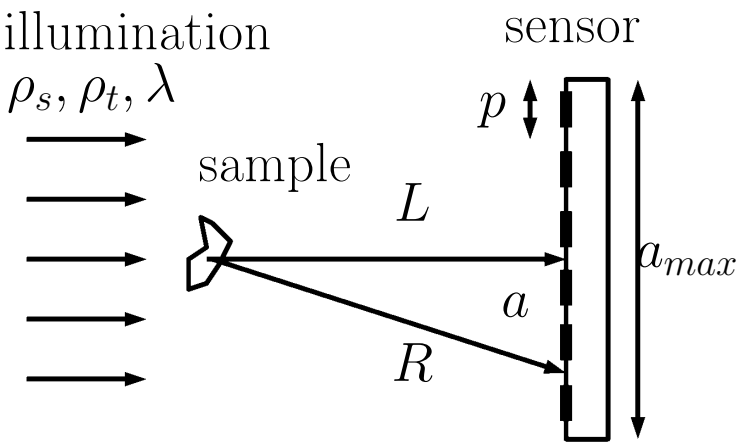

Figure 1. Schematic of a lensless in-line holographic microscope. The sample is illuminated with a plane wave with wavelength λ, having spatial coherence size of ρ_s and the temporal coherence length of ρ_t. The diffraction pattern is registered by a sensor with pitch p at a distance L .

amplitude of the field in the object plane is numerically reconstructed from the recorded hologram by solving the inverse source problem, applying backpropagation from the sensor to the sample plane. Mathematically expressed as,

$$\begin{aligned} \psi_{rec}(x,y) &= \mathcal{F}^{-1}\{\mathcal{F}\{\psi(x,y;z)\} \times \mathcal{H}(k_x,k_y;-z)\} \\ &Where \\ \mathcal{H} &= exp[-jk_0z]exp[\frac{j(k_x^2+k_y^2)z}{2k_0}] \end{aligned} \tag{2}$$

where ψ_{rec} is the reconstructed optical field of the object, $\psi(x,y;z)$ is the captured hologram , and $\mathcal{H}$ is the transfer function of free space. Our previous published work,[17] defined the optimal configuration that delivers maximum resolution to a digital inline holographic microscope. These configuration can be realized by tuning the following controlling parameters : (i) pixel size (p) of the recording sensor, (ii) linewidth $\Delta\lambda$ of the coherent illumination cone (iii) distance L between the source and the sensor plane represented by the equation below:

$$L = \frac{4p^2}{\Delta\lambda} \tag{3}$$

2.2 Flow cytometry

Flow cytometry is a technique that employs an optical-electronic detection device to analyze the physical and chemical properties of microscopic particles suspended in a liquid medium.[18] Modern micromachining methods have allowed even low-cost construction of microfluidic devices and flow channels that have had significant effect on the development of novel biomedical instrumentation in recent times. To avoid the complexity and cost of sample preparation, we investigated the possibility of detecting *S. haematobium* eggs by flowing infected patient urine without any staining protocol directly through a microchannel flow cell. Since microfluid flow is generally a low-Reynolds-number we expect a simple laminar flow and reduced system complexity.

In this work, we combine DIHM with flow cytometry to capture and detect eggs in the urine flow with a good spatial resolution and a depth of field not achievable by conventional optical microscopy. Because of its large depth of field, DIHM is ideally suited for capturing the 3-D motion of the target *S. haematobium* eggs with spatial resolution at micrometer level. To capture the stream lines of urine moving accross the defined window (the recording area of the sensor), 10 ml of urine as required by World Health Organisation diagnostic protocol, was calibrated and pumped through the channel with an injection syringe. Holograms were precisely recorded by synchronizing the urine flow rate with the frame rate of the CMOS sensor. Using developed AI models, the reconstructed images were automatically screened for the presence of *S. haematobium* eggs.

3. EXPERIMENTAL SET-UP

Ethics Statement

Eggs were obtained from gut tissue of hamsters infected with *S. haematobium* in accordance with the project license that was approved by the Dutch Central Authority for Scientific Procedures on Animals (CCD) (animal license number AVD116002017106). Hamsters were sacrificed prior and eggs were obtained after ON digestion of the gut tissue with collagenase B followed by extensive washing. The morphology and size of these gut-derived eggs represent those normally seen in urine of infected humans. Anonymized urine samples provided by willing donors who gave informed oral consent were collected and spiked with approximately 200 *S. haematobium* eggs per 12 ml of urine (1.3 ml of urine is used to flush the system and 10.7 ml). Although the eggs were harboured from the gut of infected hamsters, they adequately represents the eggs normally seen in the urine of infected humans both in size and in morphology. This makes them suitable for the experimental validation of our proposed method.

The experimental setup for DIHM is designed based on the configurations presented in,[17] following the schematic diagram of Fig. 1, A spherical wave of wavelength $\lambda = 635$ nm from a coherent point source (A S1FC635 Fiber-Coupled Laser Source from Thorlabs) illuminates the defined area of interest (AOI) of the microchannel flow. A geometrically magnified diffraction pattern at the sensor plane placed at distance L from the source is formed on a CMOS sensor with resolution of 3840×2748 pixels at a framerate of $3.2 fps$.

To efficiently record objects moving through the defined trajectory, the sensor recording area of dimension ($6.119\ mm \times 4.589\ mm$) was aligned and matched with the defined AOI of the microchannel cell. The microflow cells used in this experiment were obtained from Ibidi (a microchannel cell manufacturing company) and has a channel width of 5 mm with a depth of 0.2 mm. The channel width of 5 mm was deliberately chosen to be of smaller dimension than the recording area of the sensor. Channel depth is not a concern in this case since DIHM allows for the digital sectioning of the microchannel through image reconstruction at different planes. Given the channel depth $d(mm)$, examined volume $\mathcal{V}$, and the imaging area A and neglecting the effects of viscosity and friction for simplicity, urine flow time T_f can be approximated as:

$$T_f = \frac{\mathcal{V}}{A \times d * fps} = \frac{10^{-5}}{7.3424 \times 10^5 \times d} \tag{4}$$

Since the hologram video recording of the urine flow is memory intensive, we captured singular frames based on the exact measurement of the flow across the defined sensor window. To achieve this, we ensured a controlled flow of urine by the systematic control of the piston of the syringe with a stepper motor. This was done in such a way that the kinematics of the targets in the urine sample for example the egg (particle) motion and position can be followed at the capture rate of the image-acquisition system. Synchronizing the flow and the sensor's frame rate allows automated flow of 0.016 ml per frame. This allows the recording of 669 holographic images per urine sample of 10.7 ml, reducing the error of multiple measurements and intensive memory requirements as compared to the memory demand of video recording. The acquired holographic image frames are pre-processed and backpropagated into different planes to ensure sectioning and visualization of the whole depth of the microchannel.

Below is the summary of the procedures to obtain high-resolution DIHM reconstruction images of the target *S. haematobium* injected through the microchannels:

- Recording of holograms using a CMOS sensor. A frame rate of 0.8 frames per second which includes syringe movement, image compression and storage using the Pi 3B+ was used in the designed system.
- Recording of the microflow channel without flowing urine. The recorded image is stored as the reference image h_{ref}. The reference image contains possible manufacturing defects, dents, stains or damages on the microchannel and it is removed from subsequent hologram recordings by pixel-wise subtraction i.e., $h_1 - h_{ref}$, etc. Resultant image contains only object-related information (flowing eggs and other urine contaminants) required for processing.

- Foreground object detection by using simple algorithm to detect all moving objects recorded in the flow.The algorithm aims at detecting moving *S. haematobium* eggs and other fringe particles in the flow. The blob detection algorithm identifies potential areas of interest and thus reduces the dimension of reconstructed image.
- Backpropagation of the pre-processed hologram from the sensor to the sample plane. Different focusing distances are sampled to scan the entire microchannel depth.
- Reconstructed cropped region of interest is fed into a trained classifier for classification as *S. haematobium* eggs or not.

The complex amplitude of the field in the object plane is numerically reconstructed by backpropagating the recorded hologram from the sensor to the sample plane through a propagation distance of 3 mm. As a result of the depth of the microchannel flow cell of ($800\mu m$), egg flow is observed at different depths making reconstruction at different planes a critical factor to realize a sharp image. Since the dimensions of the *S. haematobium* eggs varies between $110-170$ μm in length and $40-70$ μm in width, we scanned the entire depth of the micro-channel using defined reconstruction distances of 400,200,100 and 50 μm. Acquired images are shown in Fig.(2 & 3).

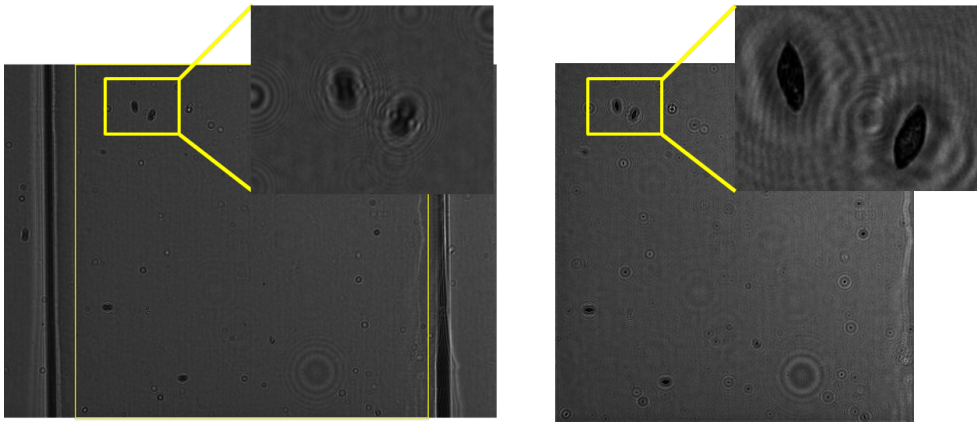

Figure 2. Registered hologram of the microchannel cell with flowing cultured sample shown on the left. The registered hologram consists of *S. haematobium* eggs flowing through the channel. The inset on the image on the left shows the registered fringe patterns of two eggs. The image at the right shows the reconstructed holographic image with the inset depicting the reconstructed images shown in the left image.

3.0.1 Image analysis and detection of eggs

The developed algorithm utilizes deep learning-based methods to create AI models for detection, analysis and classification of egg image features in the reconstructed image. The training set used for the development of our classification algorithm consisted of 3,000 randomly selected reconstructed images of *S. haematobium* eggs registered from urine spiked with eggs. The second class consist consists of patches or sub-images of background noise, and other particles presents in urine. The images in this class are classified as "Noise". To train the classification algorithm, we performed data augmentation to create synthetic variations of the images in the training data. Specifically, we used rotations (by 90° 180° and 270°) and flips of all the four orientations. By this intermediate steps, we increased the dataset size by four times, from 3000 images to 12,208 images in each class. To reduce the variation in illumination, we normalized all the pixel values from [0, 255] to [0, 1]. The dataset was split into a training set and a test set, with 70% and 30% of the images respectively. While the *S. haematobium* eggs are assigned a class label of 1, the background noise and particles were assigned a class label of 0.

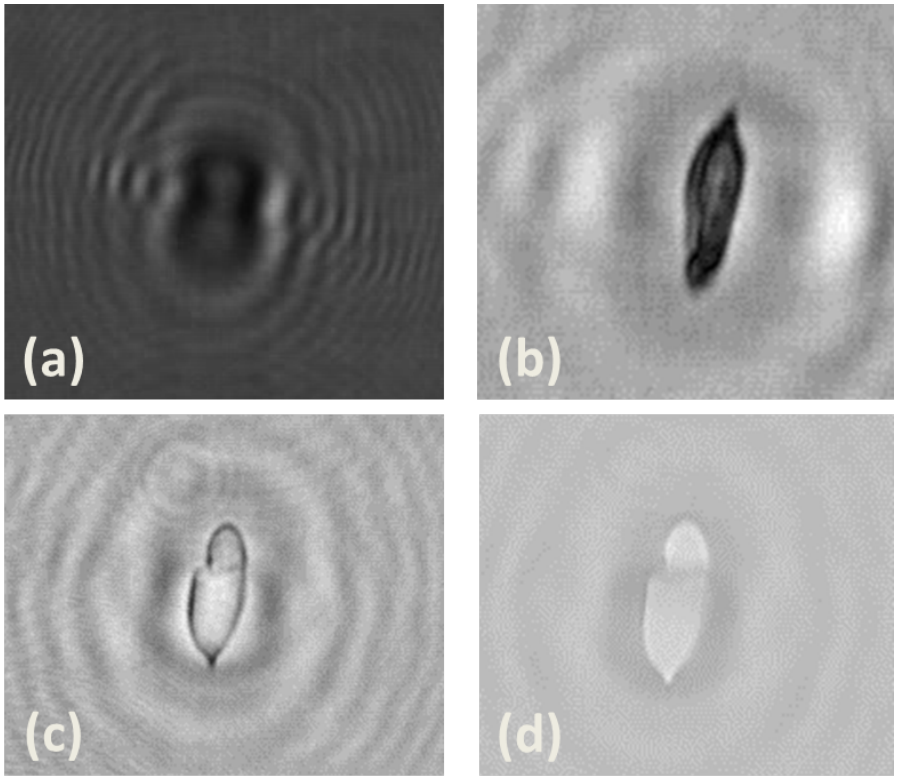

Figure 3. (a) Is the recorded hologram, (b) shows a reconstructed *S. haematobium* egg, (c) is the reconstruction image of an empty egg shell and (d) is the phase reconstruction of the empty egg shell.

4. PERFORMANCE METRICS OF ALGORITHM & RESULT

For quantitative evaluation of our classification models, we calculated the sensitivity for *S. haematobium* egg detection at the object level as the percentage of true positive (TP) divided by true positives and false negatives (FN). The specificity on an object level was estimated as the percentage of true negatives (TN) divided by the summation of true negatives and false positives (FP). In the case of true positives, the detected egg by the algorithm is confirmed as egg as compared to the ground truth. For true negatives, a non-egg detected, is actually confirmed not an egg. For false positives, what is predicted as an egg by the algorithm is actually not an egg and false negatives occurs when a detected egg is reported as a non-egg by the algorithm.

- Sensitivity provides the proportion of actual positives (eggs) that were identified correctly as eggs in a reconstructed image by the algorithm,

$$\text{Sensitivity} = \frac{\text{TP}}{\text{TP} + \text{FN}} \tag{5}$$

- Specificity measures the proportion of non-eggs that are correctly identified by the algorithm as non-eggs in the reconstructed image,

$$\text{Specificity} = \frac{\text{TN}}{\text{TN} + \text{FP}} \tag{6}$$

- The accuracy is the measure of the number of correct predictions made by the model and is defined as:

$$\text{Accuracy} = \frac{\text{TP} + \text{TN}}{\text{TP} + \text{FP} + \text{FN} + \text{TN}} \tag{7}$$

Based on the defined performance metrics, the trained model demonstrated a sensitivity of 50.6%, a specificity of 98.6% and an accuracy of 96.8%. The sensitivity and specificity tests were measured by comparing the output of our detection algorithm with the result obtained from direct expert visualization and manual counting of eggs in the reconstructed images. The sensitivity and specificity of the detection algorithm can be significantly improved with a larger training data set. This proof-of-principle study was designed to validate this methodology and estimate the performance of the detection algorithm. Diagnostic sensitivity and specificity of this technique will be measured and validated with both cultured and human samples in subsequent planned study.

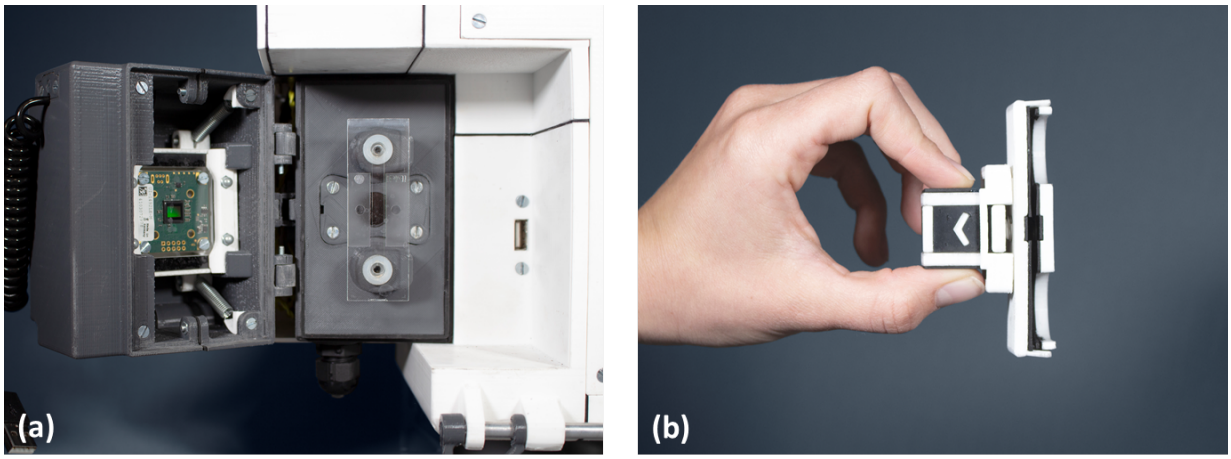

Figure 4. (a) Is the assembled parts of the imaging sensor & the micro-channel flow cell, and (b) the placement tool designed to allow for easy mounting and de-mounting of the micro-channel flow cells without damage. The prototypes were created using 3D printed laser cut parts in combination with standard off-the-shelf components.

Figure 5. (a) Is the complete diagnostic device and (b) shows the sample injection chamber where the syringe containing 12 ml of infected urine sample is mounted. The urine is pumped through through the micro-channel flow-cell by an attached stepper motor to provide accurate and consistent flow. 1.3 ml of the sample is used to flush out particles from the micro-channel flow cell.

5. SYSTEM FABRICATION AND ASSEMBLY

Design challenges to realize the first prototype of the envisioned diagnostic device include designing an appropriate embodiment of the diagnostic system and providing a suitable enclosure to mount the imaging sensor, micro-channel flow cell and the monochromatic source. The three main components were aligned on the same optical axis and mounted on 3D printed enclosures as shown in Fig 4(a). This assembly prevents stray lights and therefore reduces noise in the recorded hologram. To flow the urine sample through the micro-channel flow cell, we designed an automated sample injection system shown in Fig. 5(b). The sample injection system uses a syringe to systematically discharge the urine sample through the cells and the out-flowing urine is collected with a cup placed beneath the outlet of the flow cell. Since the position of the syringe is critical for system calibration, we placed a calibration sensor at the initial starting point (rest position) of the syringe. Persistent air bubbles in the micro-channel flow cells reduced the diagnostic accuracy. To eliminate the air bubbles, we repeatedly pushed and retracted fluids back to the syringe and thus eliminate the air bubbles by allowing them to rise into the syringe without wasting the urine sample. Also, we created an algorithm to automatically detect these bubbles and trigger this mechanism until all bubbles are completely removed. Based on the frame rate of the imaging sensor we implemented a trigger-based mode system to enable exact acquisition of the hologram at the defined area of interest. Since the image acquisition window captures approximately 0.016 ml of the sample, the stepper motor is automated and controlled to dispel the same volume of urine accordingly. After every image acquisition, the laser diode is turned-off to reduce the power consumption and to prevent overheating. To avoid low contrast holograms, we set the exposure time of the sensor at 20 ms. A complete system is shown in Fig.5(a). Major advantage of this method would be that it can be faster, high throughput (and therefore, cheaper), less labor-intensive, and maybe more sensitive if the method allows bigger volumes of urine to be tested.

6. CONCLUSION

Compared to conventional lens-based microscopes, lensless computational imaging platforms are in general simpler in hardware, compact in system design and lightweight. The essential advantage of this imaging technique is that it provides complex field information of the examined biological specimen in a wide field-of-view. In this proof of concept study, we have demonstrated a simple, less labor-intensive diagnosis of *S.haematobium* infection using a combination of a lensless in-line holographic microscope with flow cytometry technique. Our proposed method requires no sample preparation method and can therefore potentially alleviate the cost and complexity associated with conventional sample preparation technique. Computer-assisted diagnosis is achieved using low computationally expensive feature extraction binary classifier combined with simple image processing technique. The automated egg detection algorithm could potentially reduce the intensive manual labour, and the usual need for human expert associated with the conventional diagnostic methods. However, the current limitation of this technique is that over 650 holographic images are registered per sample. Required computational effort and time required to process this large amount of data is critical. For example, an average of 3.5 hours is required for the processing of 650 images registered from the flow of one 12 ml sample. The reported diagnostic time per sample is too high as compared to the current standard manual microscopy diagnostic methods that requires less than 15 minutes per test. For this method to find contributory relevance as -a point-of-care diagnostics in a resource-poor setting, the image reconstruction and egg detection algorithm must be optimized for improved time efficiency and accuracy. Current effort is ongoing in our laboratory to speed up the reconstruction and egg detection time. System performance in terms of sensitivity and specificity is also being improved. Preliminary results obtained are promising and a larger field study is being planned to validate the developed methods with human samples. We hope that our proposed methodology will complement existing point-of-need diagnostic devices for the detection of *S. haematobium* eggs in urine samples collected in resource limited settings.

ACKNOWLEDGMENTS

The authors acknowledge and appreciate the support of G-Young Van from TU Delft, Netherlands and Mirte Vendel from AIDX Medical B.V. G.Vdovine is partly sponsored by Flexible Optical BV and T. Agbana's research is funded by Delft Global Initiative of TU Delft. Part of the research described has been funded by the NWO-WOTRO SDG programme grant INSPiRED (W 07.30318.009).

REFERENCES

[1] Utzinger, J., Becker, S. L., van Lieshout, L., van Dam, G. J., and Knopp, S., "New diagnostic tools in schistosomiasis," *Clinical microbiology and infection* **21**(6), 529–542 (2015).

[2] Knopp, S., Becker, S. L., Ingram, K. J., Keiser, J., and Utzinger, J., "Diagnosis and treatment of schistosomiasis in children in the era of intensified control," *Expert review of anti-infective therapy* **11**(11), 1237–1258 (2013).

[3] Gray, D. J., Ross, A. G., Li, Y.-S., and McManus, D. P., "Diagnosis and management of schistosomiasis," *Bmj* **342**, d2651 (2011).

[4] Gryseels, B., Polman, K., Clerinx, J., and Kestens, L., "Human schistosomiasis," *The Lancet* **368**(9541), 1106–1118 (2006).

[5] Bogoch, I. I., Coulibaly, J. T., Andrews, J. R., Speich, B., Keiser, J., Stothard, J. R., N'goran, E. K., and Utzinger, J., "Evaluation of portable microscopic devices for the diagnosis of schistosoma and soil-transmitted helminth infection," *Parasitology* **141**(14), 1811–1818 (2014).

[6] Rajchgot, J., Coulibaly, J. T., Keiser, J., Utzinger, J., Lo, N. C., Mondry, M. K., Andrews, J. R., and Bogoch, I. I., "Mobile-phone and handheld microscopy for neglected tropical diseases," *PLoS neglected tropical diseases* **11**(7), e0005550 (2017).

[7] Coulibaly, J. T., Ouattara, M., D'Ambrosio, M. V., Fletcher, D. A., Keiser, J., Utzinger, J., N'Goran, E. K., Andrews, J. R., and Bogoch, I. I., "Accuracy of mobile phone and handheld light microscopy for the diagnosis of schistosomiasis and intestinal protozoa infections in côte d'ivoire," *PLoS neglected tropical diseases* **10**(6), e0004768 (2016).

[8] Ephraim, R. K., Duah, E., Cybulski, J. S., Prakash, M., D'Ambrosio, M. V., Fletcher, D. A., Keiser, J., Andrews, J. R., and Bogoch, I. I., "Diagnosis of schistosoma haematobium infection with a mobile phone-mounted foldscope and a reversed-lens cellscope in ghana," *The American journal of tropical medicine and hygiene* **92**(6), 1253–1256 (2015).

[9] Agbana, T. E., Diehl, J.-C., van Pul, F., Khan, S. M., Patlan, V., Verhaegen, M., and Vdovin, G., "Imaging & identification of malaria parasites using cellphone microscope with a ball lens," *PloS one* **13**(10), e0205020 (2018).

[10] Switz, N. A., D'Ambrosio, M. V., and Fletcher, D. A., "Low-cost mobile phone microscopy with a reversed mobile phone camera lens," *PloS one* **9**(5), e95330 (2014).

[11] Mudanyali, O., Tseng, D., Oh, C., Isikman, S. O., Sencan, I., Bishara, W., Oztoprak, C., Seo, S., Khademhosseini, B., and Ozcan, A., "Compact, light-weight and cost-effective microscope based on lensless incoherent holography for telemedicine applications," *Lab on a Chip* **10**(11), 1417–1428 (2010).

[12] Lee, M., Yaglidere, O., and Ozcan, A., "Field-portable reflection and transmission microscopy based on lensless holography," *Biomedical optics express* **2**(9), 2721–2730 (2011).

[13] Xu, W., Jericho, M., Meinertzhagen, I., and Kreuzer, H., "Digital in-line holography for biological applications," *Proceedings of the National Academy of Sciences* **98**(20), 11301–11305 (2001).

[14] Ozcan, A. and McLeod, E., "Lensless imaging and sensing," *Annual review of biomedical engineering* **18**, 77–102 (2016).

[15] Garcia-Sucerquia, J., Xu, W., Jericho, S. K., Klages, P., Jericho, M. H., and Kreuzer, H. J., "Digital in-line holographic microscopy," *Applied optics* **45**(5), 836–850 (2006).

[16] Linder, E., Grote, A., Varjo, S., Linder, N., Lebbad, M., Lundin, M., Diwan, V., Hannuksela, J., and Lundin, J., "On-chip imaging of schistosoma haematobium eggs in urine for diagnosis by computer vision," *PLoS neglected tropical diseases* **7**(12), e2547 (2013).

[17] Agbana, T. E., Gong, H., Amoah, A. S., Bezzubik, V., Verhaegen, M., and Vdovin, G., "Aliasing, coherence, and resolution in a lensless holographic microscope," *Optics letters* **42**(12), 2271–2274 (2017).

[18] Shapiro, H. M., [*Practical flow cytometry*], John Wiley & Sons (2005).